

# Effects of Inhibition and Dendritic Saturation in Simulated Neocortical Pyramidal Cells

PAUL C. BUSH AND TERRENCE J. SEJNOWSKI

Howard Hughes Medical Institute and Computational Neurobiology Laboratory, Salk Institute, La Jolla 92037; and University of California at San Diego, La Jolla, California 92093

## SUMMARY AND CONCLUSIONS

1. We have used compartmental models of reconstructed pyramidal neurons from layers 2 and 5 of cat visual cortex to investigate the nonlinear summation of excitatory synaptic input and the effectiveness of inhibitory input in countering this excitation.

2. In simulations that match the conditions of a recent experiment, dendritic saturation was significant for physiological levels of synaptic activation: a compound excitatory postsynaptic potential (EPSP) electrically evoked during a depolarization caused by physiological synaptic activation was decreased by up to 80% compared with an EPSP evoked at rest.

3. Synaptic inhibition must be coactivated with excitation to quantitatively match the experimental results. The experimentally observed coactivation of inhibition with excitation produced additional current shunts that amplified the decrease in test EPSP amplitude. About 30% of the experimentally observed decrease in EPSP amplitude was caused by decreases in input resistance ( $R_{in}$ ) due to synaptic conductance changes; a reduced driving force accounted for the remaining decrease.

4. The amount of inhibition was then increased by nearly an order of magnitude, to  $\sim 10\%$  of the total number of inhibitory synapses on a typical cortical pyramidal cell. The sustained firing of this many inhibitory inputs was sufficient to completely suppress the firing of a neuron receiving strong excitatory input. However, this level of inhibition produced a very large reduction in  $R_{in}$ . Such large reductions in  $R_{in}$  have not been observed experimentally, suggesting that inhibition in cortex does not act to veto (shunt) strong, *sustained* excitatory input (of order 100 ms).

5. We propose instead that strong, *transient* activation ( $< 10$  ms) of a neuron's inhibitory inputs, sufficient to briefly prevent firing, is used to shape the temporal structure of the cell's output spike train. Specifically, cortical inhibition may serve to synchronize the firing of groups of pyramidal cells during optimal stimulation.

## INTRODUCTION

The traditional function assigned to inhibition in cortex is to oppose excitation, acting to veto or shape the response of cortical cells by negating inappropriate excitation (Koch et al. 1987). Evidence for this view was provided by blocking inhibition with bicuculline and observing a decrease in the response selectivity of cortical neurons (Sillito 1975). However, theoretical studies (Koch et al. 1990) have shown that inhibition strong enough to veto (shunt) significant amounts of excitatory current should produce measurable decreases in  $R_{in}$  of the neuron in question. Such decreases in  $R_{in}$  have never been seen in vivo when cortical neurons do not respond to nonpreferred stimuli (Berman et al. 1991; Douglas et al. 1988), and electrically evoked thala-

mocortical excitatory postsynaptic potentials (EPSPs) are not reduced in amplitude during visual stimulation at the nonpreferred orientation (Ferster and Jagadeesh 1992). These results have led to the conclusion that cortical neurons receive neither excitatory nor inhibitory input in response to nonpreferred stimuli (Berman et al. 1991). This conclusion is supported by results showing that both the excitation and the inhibition that a cortical neuron receives are tuned to the preferred orientation (Ferster 1986).

Thus it is becoming clear that the role of cortical inhibition is more complex than a veto of sustained, untuned excitation. A number of other functions for inhibition have been proposed: recent physiological experiments using dual gratings (Bonds 1989) have suggested that a general, nonselective inhibition acts to normalize cortical responses. This idea receives direct anatomic support from the recent demonstration that large basket cells send (inhibitory) inputs to regions representing all orientations, not just iso- or cross-orientations (Kisvardy and Eysel 1993). Douglas and Martin have proposed that cortical inhibition acts to increase the threshold of target neurons and gate intracortical reexcitation (Douglas and Martin 1992). To remain in a state that is sensitive to inputs, the excitation and inhibition to a cortical cell should be balanced (T. A. Bell, Z. F. Mainen, and T. J. Sejnowski, unpublished data).

To study these issues we have simulated a recent experiment (Ferster and Jagadeesh 1992) that used in vivo whole-cell patch recording of neocortical neurons to study interactions between synaptic inputs. We have applied a compartmental model to the data of Ferster and Jagadeesh (1992) and shown that they are consistent with nonlinear interactions occurring in dendrites between excitatory inputs alone and between excitatory and inhibitory inputs. The same model was then used to determine conditions under which inhibition can prevent the firing of a neuron receiving synaptic excitation that is strong enough to cause it to discharge at high rates, and how much  $R_{in}$  would change under these conditions. Our results, consistent with the experimental data, lead to a hypothesis in which inhibition is strongly activated during periods of maximum excitation, yet not in a manner that causes a suppression of the firing response.

## METHODS

Simulations were performed with the use of standard techniques for compartmental models of branching dendritic trees (Rall 1964); two digitized horseradish peroxidase (HRP)-filled

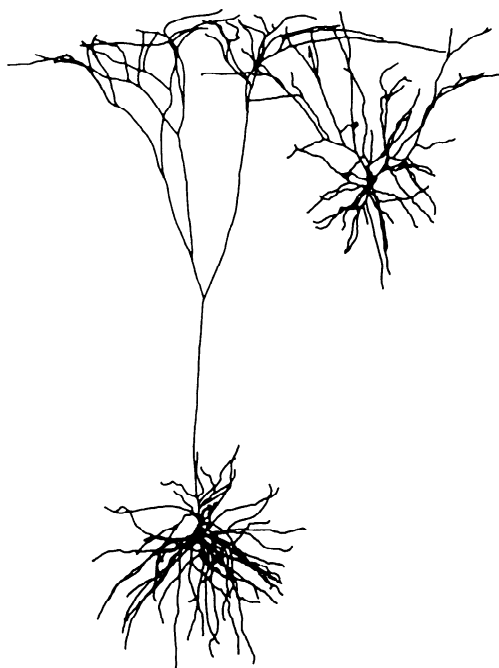


FIG. 1. Drawings of reconstructed horseradish peroxidase (HRP)-filled layer 2 (right) and layer 5 (left) pyramidal cells. Scale bar 100  $\mu\text{m}$ .

pyramidal cells from layers 2 and 5 of cat visual cortex (Koch et al. 1990) were modeled (Fig. 1), each having  $\sim 400$  coupled cylindrical compartments containing only resistive and capacitive elements. The simulator CABLE (Hines 1989), running on a MIPS Magnum 3000/33, required  $\sim 1$  min of computation to simulate 100 ms of real time.

### Passive parameters

Appropriate values of the passive parameters (specific membrane resistance,  $R_m$ ; specific membrane capacitance,  $C_m$ ; and specific axial resistance,  $R_i$ ) were selected:  $C_m$  for neuronal membrane has a long-established value of  $1 \mu\text{F}/\text{cm}^2$  (Jack et al. 1975). The accepted value of  $R_i$ , at least in the mammalian CNS, has recently been revised upward from its traditional value of  $\sim 70 \Omega\text{cm}$  for a number of reasons. 1) Voltage responses to brief current pulses could not be modeled accurately with a small  $R_i$  (Segev et al. 1992; Shelton 1985; Stratford et al. 1989). 2) When modeling cerebellar Purkinje cells, a larger  $R_i$  was necessary to produce significant attenuation of action potentials as they invade the dendritic tree (Bush and Sejnowski 1991). 3) A large  $R_i$  was needed to explain the observed somatic to dendritic input conductance ratio and steady-state voltage attenuation of Purkinje cells [for a discussion of this issue see Shelton (1985)]. The value chosen for  $R_i$  in this study was  $200 \Omega\text{cm}$  (Bernander et al. 1991; Segev et al. 1992; Shelton 1985; Stratford et al. 1989).

Once  $R_i$ ,  $C_m$ , and the morphology have been fixed, the value chosen for  $R_m$  will determine  $R_{in}$ , the time constant,  $\tau_m$ , and the length constant,  $\lambda$ , of the cell. Recent results using whole-cell patch electrodes and  $\text{Cs}^+$ -filled sharp electrodes have increased the estimate of  $R_m$  from its traditional value of  $5\text{--}10 \text{ k}\Omega\text{cm}^2$  to a value of  $50\text{--}100 \text{ k}\Omega\text{cm}^2$  (Andersen et al. 1990; Major et al. 1990; Spruston and Johnston 1992; Staley et al. 1992), giving  $R_{in}$ s in the range of a  $\text{G}\Omega$ . However, these results were not obtained in vivo, where the effect of background synaptic activity is such that a neuron with a  $R_m$  of  $100 \text{ k}\Omega\text{cm}^2$  can have an effective  $R_{in}$  as low as  $20 \text{ M}\Omega$  and an effective  $\tau_m$  of  $\sim 20$  ms when part of an active in vivo circuit (Bernander et al. 1991; Rapp et al. 1992). The background synaptic input decreases the effective average  $R_m$  of

an in vivo neuron in a way that can be accurately taken into account by simply using a lower value for the effective  $R_m$  in the model (Barrett and Crill 1974; Bernander et al. 1991; Holmes and Woody 1989). A sample of 25 visual cortical neurons recorded with the use of sharp electrodes in vivo had  $R_{in}$ s ranging from 10 to  $153 \text{ M}\Omega$  (mean  $69 \text{ M}\Omega$ ) (Douglas et al. 1991). Two independent measurements of visual cortical neurons recorded with use of whole-cell patch electrodes in vivo had  $R_{in}$ s ranging from 50 to  $200 \text{ M}\Omega$  (Ferster and Jagadeesh 1992) and 50 to  $150 \text{ M}\Omega$  (Pei et al. 1991). The range of  $R_{in}$  values reported by these studies is similar. Values for  $R_{in}$  of  $50\text{--}150 \text{ M}\Omega$  are closer to values obtained from the best sharp electrode in vitro recordings (Tanaka et al. 1991) than to the hundreds of  $\text{M}\Omega$  obtained by the use of whole-cell clamping in vitro.

With a  $C_m$  of  $1 \mu\text{F}/\text{cm}^2$  and  $R_i$  of  $200 \Omega\text{cm}$ , we found that using a value of  $20 \text{ k}\Omega\text{cm}^2$  for  $R_m$  produced  $R_{in}$ s for the model layer 5 and layer 2 pyramidal cells of 45 and  $110 \text{ M}\Omega$ , respectively. The layer 2 cell had a greater  $R_{in}$  because it was smaller. With these parameters (the standard model) both model cells have a dendritic  $\tau_m$  of 20 ms, which is a typical value for neocortical cells (Bernander et al. 1991).

Although we believe that these values produce an accurate model of the in vivo neocortical pyramidal neuron, there is still considerable controversy surrounding "correct" values for the passive parameters  $R_m$  and  $R_i$ . Consequently, all simulations were repeated with the use of values for  $R_i$  of 70, 200, and  $500 \Omega\text{cm}$  and values for  $R_m$  of 5, 20, and  $100 \text{ k}\Omega\text{cm}^2$ . We focus on results obtained with the standard model (the default for all simulations), which we believe to be the most accurate fit to a functioning pyramidal cell, but we also present and discuss results obtained by the use of the full range of values for  $R_m$  and  $R_i$ . In general, we found only a quantitative, rather than a qualitative, difference between simulations using different parameter values, and none of our conclusions depend on precise values.

### Synaptic conductances

EPSPs and inhibitory postsynaptic potentials (IPSPs) in our models were simulated as alpha function conductance changes with a peak amplitude of  $0.5 \text{ nS}$  and a time to peak of 1 ms. EPSPs had a reversal potential of 0 mV and IPSPs a reversal potential of  $-70 \text{ mV}$  (Connors et al. 1988; McCormick 1989). These parameters were chosen because they produced EPSPs at the soma with the same time course and amplitude as those observed experimentally (Mason et al. 1991; Thomson et al. 1988). Some simulations were done with synapses on explicitly modeled spines. In these cases we used the same two-compartment model spine morphology as Qian and Sejnowski (1989), with spine neck dimensions  $1 \times 0.1 \mu\text{m}$  and head  $0.69 \times 0.3 \mu\text{m}$ . Trains of EPSPs or IPSPs were modeled according to a Poisson distribution with a mean frequency that is stated for each case. The resting membrane potential was  $-65 \text{ mV}$ .

### Active conductances

For some simulations active conductances were placed at the soma to generate adapting trains of action potentials, as observed in regular-firing cortical neurons (McCormick et al. 1985). The action potential was mediated by fast sodium and potassium conductances ( $g_{\text{Na}} + g_{\text{Kd}}$ ). A high-threshold calcium conductance ( $g_{\text{Ca}}$ ), activated by each spike, introduced calcium into the cell. Intracellular calcium accumulated in the soma compartment and decayed exponentially to its resting value with a time constant of 20 ms (Traub et al. 1991). A slow calcium-sensitive potassium conductance ( $g_{\text{Kca}}$ ) was included to produce the adaptation of firing rate. All the conductances used the Hodgkin-Huxley-like kinetics parameters developed by Borg-Graham (Borg-Graham 1987), except for  $g_{\text{Kca}}$ , which had an activation rate equal to 200

TABLE 1. Parameters for active conductances

Channel	$E_r$ , mV	$g$ , mS/cm <sup>2</sup>	$z$	$g$	$a_0, b_0$	$V_{1/2}$	$t_{min}$ , ms	$T$ , °C	$n$
Na, m	45	40	4.3	0.7	4.2	-38	0.05	37	3
Na, h			-6	0.5	0.2	-42	0.5	37	1
Kd	-90	30	3	0.7	0.03	-35	1.0	24	4
Ca	NA	0.6	6	0.7	1	-15	0.1	37	1
K <sub>Ca</sub>	-90	10				See text			

NA, not applicable.

times the intracellular calcium concentration (in ms<sup>-1</sup>) and a deactivation rate equal to the reciprocal of the activation rate. The implementation of our kinetic scheme follows that of Lytton and Sejnowski (1991). Briefly, each ionic current,  $I$ , was calculated from

$$I = gm^n h(V - E_r) \quad (1)$$

where  $g$  is maximal conductance,  $m$  is the activation variable,  $n$  is the exponent,  $h$  is the inactivation variable ( $g_{Na}$  only),  $V$  is membrane potential, and  $E_r$  is the reversal potential of the ion concerned. The calcium current was calculated with the use of the Goldman-Hodgkin-Katz equation (Hille 1984), with  $g_{Ca}$  the calcium permeability. The time- and voltage-dependent variable,  $m$ , converged on a steady-state value,  $m_{inf}$ , given by

$$m_{inf} = \alpha_m / (\alpha_m + \beta_m)$$

with a time constant,  $t_m$ , given by

$$t_m = 1 / (\alpha_m + \beta_m)$$

The rate constants  $\alpha_m$  and  $\beta_m$  were defined by the equations

$$\alpha_m = a_0 \exp[zg(V - V_{1/2})F/RT]$$

$$\beta_m = b_0 \exp[-z(1-g)(V - V_{1/2})F/RT]$$

where  $F$  is the Faraday constant,  $R$  is the gas constant, and  $T$  is temperature. The kinetics of each channel was determined by the values assigned to the parameters  $a_0$ ,  $b_0$ ,  $z$ ,  $g$ , and  $V_{1/2}$ . A similar set of equations governed the inactivation variable,  $h$ , and its steady-state value,  $h_{inf}$ . The values of all the parameters used in the model arc shown in Table 1.

## RESULTS

### Dendritic saturation

Dendrites have a much higher input impedance than the soma (Rinzel and Rall 1974); thus even single EPSPs can produce significant local depolarization and reduce the driving force on simultaneous and subsequent EPSPs on the same dendritic branch. In addition, synaptic conductances add to the resting membrane conductance of the neuron (Barrett and Crill 1974; Bernander et al. 1991; Holmes and Woody 1989; Rapp et al. 1992) (see METHODS). This effective decrease in  $R_m$  and increase in  $\lambda$  also results in reduced depolarizations for simultaneous and subsequent EPSPs. We refer to these two phenomena collectively as the dendritic saturation effect, although the term "saturation" does not necessarily imply that the membrane is at the synaptic reversal potential or that  $R_m$  has been effectively reduced to zero.

There is some direct experimental evidence for saturation during synaptic activation under physiological conditions. Ferster and Jagadeesh (1992) have demonstrated that the size of an EPSP evoked in visual cortical cells by electrical stimulation of the lateral geniculate nucleus

(LGN) was reduced during depolarizations caused by visual stimulation compared with its size at the resting potential. The reduction in EPSP size was proportional to the somatic depolarization caused by the visual stimulation. Thus an EPSP that peaked at  $\sim 6$  mV at rest was reduced to  $< 1$  mV when the cell was depolarized from a resting potential of  $-60$  mV to a potential of  $-40$  mV by visual stimulation (Fig. 3A) (Ferster and Jagadeesh 1992).

Ferster and Jagadeesh interpreted their results as evidence that the synaptic sites (dendrites) were significantly more depolarized than the soma during synaptic activation of the cell, thus producing saturation by the process described above. We have tested this hypothesis by simulating their experiment, and the results are shown in Figs. 2 and 3. The model layer 2 pyramidal cell was used because its morphology (Fig. 1) is reasonably close to that of the putative layer 4 spiny stellate cells that Ferster and Jagadeesh studied. A constant current of  $-0.1$  nA was injected starting at 30 ms to prevent firing during the synaptic activation, as in the experiments of Ferster and Jagadeesh. Visual stimulation was simulated by 70 excitatory synapses placed randomly on the basal/oblique dendrites, activated by a Poisson process at some mean frequency (for example, 50 Hz) starting at 80 ms. Thirty-five additional excitatory synapses were placed on the same dendritic segments as the initial 70 and were given a single simultaneous stimulation at 5 ms and again at 150 ms. The firing of these 35 synapses repre-

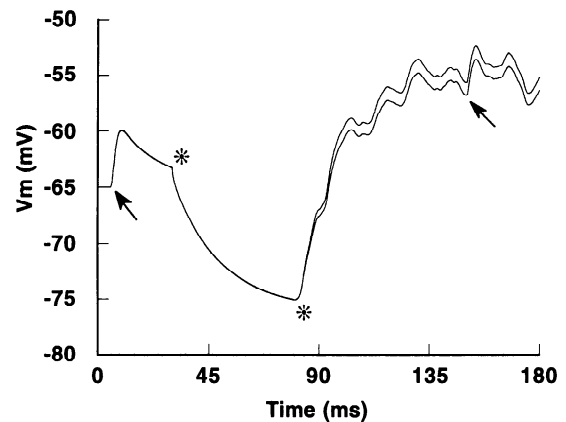


FIG. 2. Simulation of reduction in amplitude of excitatory postsynaptic potential (EPSP) by synaptic activity. Somatic membrane potential ( $V_m$ ) during simulation of model layer 2 pyramidal cell. A constant current of  $-0.1$  nA is injected into the soma at  $t = 30$  ms to prevent firing (1st \*), then 70 excitatory synapses are activated at a mean frequency of 50 Hz to simulate visual stimulation (2nd \*). Thirty-five additional excitatory synapses are given a simultaneous stimulus to produce a control (1st x) and test (2nd x) EPSP. The amplitude of the test EPSP is significantly reduced with respect to the control. Top trace: result of simulation with all excitatory synapses directly on dendritic shafts. Bottom trace: result of simulation with all synapses on the heads of dendritic spines (see METHODS).

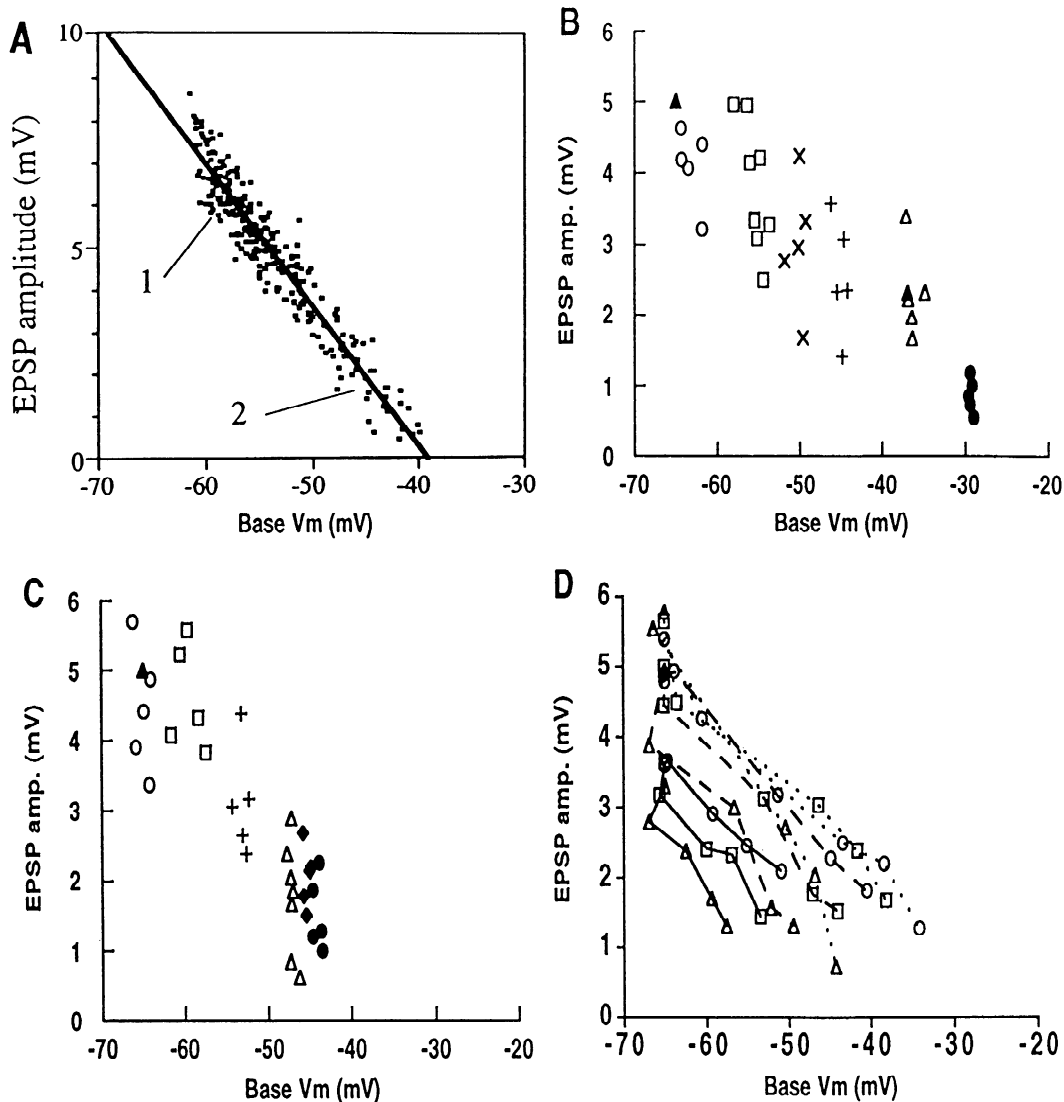


FIG. 3. Dendritic saturation during physiological synaptic activation. *A*: experimental data: peak amplitude of the test EPSP plotted against  $V_m$  just before the EPSP occurred while the visual stimulus was at the optimal orientation for the cell. Arrow 1 indicates control EPSP (before stimulation), arrow 2 indicates test EPSP (at peak of visual response) [reproduced by permission (Ferster and Jagadeesh 1992)]. *B*: simulation of the experiment in *A*, as detailed in Fig. 2. Peak amplitude of the test EPSP plotted against  $V_m$  just before the EPSP occurred, for a variety of firing frequencies of the 70 excitatory synapses.  $\blacktriangle$ , 0 Hz;  $\circ$ , 25 Hz;  $\square$ , 50 Hz;  $\times$ , 75 Hz;  $+$ , 100 Hz;  $\triangle$ , 200 Hz;  $\blacklozenge$ , 300 Hz;  $\bullet$ , 400 Hz. The amplitude of the EPSP decreased linearly with  $V_m$ . *C*: concurrent inhibition is included in the simulation (33 inhibitory synapses at twice frequency of excitatory synapses). *D*: simulations in *C* repeated for  $R_m$  values of 5  $k\Omega cm^2$  (—), 20  $k\Omega cm^2$  (---), and 100  $k\Omega cm^2$  ( $\cdots$ ) and  $R_i$  values of 70 ( $\circ$ ), 200 ( $\square$ ), and 500 ( $\triangle$ )  $\Omega cm$ . Data plotted for excitatory input frequencies of 0, 25, 100, 200, and 400 Hz. Each point is the average of 5 trials.

sented the effects of electrical stimulation of the LGN: the first stimulation gave a control EPSP, the second, occurring during "visual stimulation," gave a test EPSP. Different trials using a different seed for the random number generator produced Poisson-distributed trains of EPSPs. One such trial is shown in Fig. 2 (*top trace*). The test EPSP was significantly reduced with respect to the control EPSP (by 34% in this case).

#### Effects of spines

The saturation effect underlying the reduction in EPSP amplitude was dependent on the membrane potential at the synaptic site. Excitatory synapses on real pyramidal cells

are made onto spines, not onto dendritic shafts. It was conceivable that the small dimensions, and hence higher input resistance, of a spine head relative to that of a dendritic shaft might lead to greater saturation effects for EPSPs on spines versus shafts (Segev and Rall 1988). Consequently, we performed some simulations with excitatory synapses on spine heads rather than dendritic shafts. For a single 0.5-nS EPSP, there was very little difference in the depolarization recorded at the soma for a synapse on the head of a spine versus on the dendritic shaft; the activation of synapses on spines produced a somatic peak amplitude >90% of that from synapses on the shaft. Significant saturation of single EPSPs due to the passive properties of the spine (Douglas and Martin 1990b) was only observed if the peak

EPSP conductance was increased to several nanosiemens. EPSPs produced by these conductance changes were larger than those typically observed in neocortical pyramidal cells (Mason et al. 1991).

To simulate the experiment of Ferster and Jagadeesh with spines explicitly included, 70 spines were placed on the 70 basal dendritic compartments chosen above, then 35 more were added to provide the control and test EPSPs. The result of the simulation with all excitatory synapses on spines (*bottom trace*, Fig. 2) was not significantly different from that with all excitatory synapses directly on dendritic shafts (*top trace*). The presence of spines did not make a difference over the full range of visual stimulation frequencies used. We also found very little difference between simulations using 35 0.2-nS test synapses and those using 14 0.5-nS test synapses.

Although spines may be of great significance in some contexts (Zador et al. 1990), we were only concerned here with ensuring that our results would not be significantly affected by placing all the excitatory synapses on dendritic shafts rather than on spine heads. Figure 2 shows that this approach is justified. For this reason, in the remaining simulations spines were not included.

#### *Effect of excitation on saturation*

Figure 3B shows the results of multiple trials at different frequencies of visual stimulation. Higher frequencies of excitatory input produced greater somatic depolarization, as would occur in a cell as the visual stimulus was presented at increasingly optimal values of orientation, velocity, and direction. The peak amplitude of the EPSP is plotted against the somatic membrane potential ( $V_m$ ) just before the EPSP occurs. As in the experimental data (Fig. 3A), the amplitude of the evoked EPSP decreased linearly with  $V_m$ . The dendrites were depolarized to between  $-25$  and  $-20$  mV during maximal synaptic activation, which means that the EPSP driving force was reduced by  $\sim 60\%$ . Because the test EPSP was reduced by  $\sim 80\%$  during maximal synaptic activation (Fig. 3B), a reduction in EPSP size of  $\sim 20\%$  was due to a reduction in  $R_{in}$  caused by the excitatory synaptic input. A more detailed, quantitative description of changes in  $R_{in}$  during synaptic activation is presented in the last section of RESULTS.

The results shown in Fig. 3B provide a qualitative match to those of Ferster and Jagadeesh, but the difference between the level of somatic and dendritic depolarization in the model was not great. In addition, the slope of the relationship between EPSP height and somatic  $V_m$  was not as steep as in the experimental data: the abscissa intercept (EPSP reduced to 0 mV) is about  $-40$  mV in the experimental results (Fig. 3A) and  $-25$  mV in Fig. 3B. Ferster and Jagadeesh report that visual cortical cells cannot be depolarized by  $>20$  mV from rest by visual stimulation (Ferster and Jagadeesh 1992). For our model cell (resting potential  $-65$  mV), this corresponds to complete saturation at a somatic  $V_m$  of  $-45$  mV.

#### *Effect of inhibition on saturation*

The difference between our simulations of dendritic saturation and the experimental results could be due to the omission of inhibitory input in the simulation. Recent stud-

ies (Berman et al. 1991; Douglas et al. 1988; Ferster and Jagadeesh 1992) have indicated that inhibitory input to visual cortical cells is weak during nonpreferred responses and is strongly correlated with the degree of activation of the excitatory cells (Ferster 1986; Somers et al. 1993). This fits with anatomic evidence that spiny excitatory cells make direct contacts with inhibitory cells, which then make direct contacts back onto the same excitatory population (Douglas and Martin 1991). We repeated the simulation described above, this time including 33 inhibitory synapses, 12 on the soma and 21 on the preterminal basal/oblique dendrites. This is the pattern of innervation characteristic of basket cells, the most common inhibitory cell type in cortex (Martin 1988). Inhibitory (smooth) cells fire at much higher rates than pyramidal cells (McCormick et al. 1985); therefore inhibitory synapses were activated at a mean frequency twice that of the excitatory synapses. Figure 3C shows the results of including inhibition in the simulation. The EPSP/somatic  $V_m$  slope is steeper, with an abscissa intercept of about  $-35$  mV. This is much closer to the experimental data of Ferster and Jagadeesh (Fig. 3A). Dendrites were depolarized to about  $-30$  mV during maximal synaptic activation, less than in the excitation-alone case, yet the EPSP/somatic  $V_m$  slope is steeper with inhibition. A dendritic depolarization to around  $-30$  mV reduced the EPSP driving force by  $\sim 50\%$ . Test EPSPs were reduced in amplitude by up to 80%, so the remaining 30% must be due to decreases in  $R_{in}$  caused by the excitatory and inhibitory synaptic conductance changes (see DISCUSSION). There may also be some contribution to the reduction in  $R_{in}$  and hence EPSP amplitude from intrinsic subthreshold voltage-dependent conductances during the experiments of Ferster and Jagadeesh. The simulations of Fig. 3 did not include voltage-dependent conductances, so we cannot evaluate the extent of this contribution, but the simulations of Bernander et al. (1991) indicate that it is likely to be relatively small.

Ferster and Jagadeesh (1992) focused on reduction in driving force as the explanation for the decreases in evoked EPSP amplitude that they observed, but we found that decreases in  $R_{in}$  (decrease in effective  $R_m$ ) due to excitatory inputs made a significant contribution. Furthermore, additional current shunts due to inhibitory synaptic activity must be included to produce an accurate fit to the experimental data. The data in Fig. 3C fall along a straight line because the major component of the saturation effect is due to the linear reduction in driving force. The contribution from increased membrane conductance, which would produce a concave (hyperbolic) curve, is masked by the driving force effect and the variance in the data. When inhibition was included in the simulation, the soma could not be depolarized past  $-45$  mV by the firing of the 70 excitatory synapses, which is the limit of depolarization obtainable with optimal visual stimulation reported by Ferster and Jagadeesh (1992).

Figure 3D shows that the decrease in test EPSP amplitude due to dendritic saturation is stable across a wide range of values for  $R_m$  and  $R_i$ . The rate of decrease of EPSP amplitude with somatic  $V_m$  was constant over the full parameter range.

Figure 4 displays in higher resolution dendritic (---)

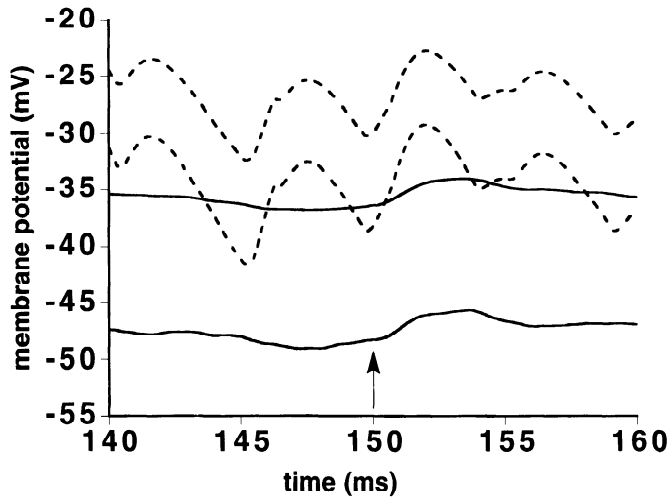


FIG. 4. Effect of inhibition on dendritic saturation at low input rates. Dendritic (---) and somatic (—) membrane potentials during the application of the test EPSP ( $\uparrow$ ) with (*bottom traces*) and without (*top traces*) inhibitory input are shown.

and somatic (—) membrane potentials at the time of the test EPSP ( $\uparrow$ ) for synaptic input with (*bottom traces*) and without (*top traces*) inhibition. A number of important points are illustrated: because of a higher  $R_{in}$ , the dendrite is more depolarized than the soma (and this dendrite is less depolarized than most), with larger voltage fluctuations due to the influence of individual postsynaptic potentials. The dendrite is less hyperpolarized than the soma by the inhibition because the inhibitory synapses are proximal and act by shunting current that passes from the dendrites to the soma. The effect of inhibition is to increase the slope of the test EPSP/somatic  $V_m$  graph (Fig. 3C), so at the low input rate shown here inhibition causes a small *increase* in the size of the test EPSP by slightly hyperpolarizing the membrane thus increasing the excitatory synaptic driving force.  $\gamma$ -Aminobutyric acid-A ( $GABA_A$ ) inhibition, the type we are modeling here, acts by increasing membrane conductance rather than directly hyperpolarizing the membrane, because its reversal potential is close to the resting membrane potential. The driving force for inhibitory chloride conductance only exists when there is depolarization produced by excitatory synaptic input (silent inhibition). At higher firing rates, when the inhibitory conductance is large, the small increase in excitatory driving force caused by the hyperpolarization (which is minimized at the site of the excitatory synapses by the spatial separation of the sources of excitatory and inhibitory input, mentioned above) is more than offset by the shunting effect of the inhibition, and the test EPSP is decreased in size (Fig. 3C).

The soma could still be depolarized by 20 mV from rest even when the 33 inhibitory synapses are firing at their maximum rate (Fig. 3). This indicates that firing of the postsynaptic cell would persist despite significant inhibition. This seems to support the conclusion of Douglas and Martin (1990a), who simulated the effect of a maintained inhibitory conductance on the firing rate of a simplified model neuron driven by intrasomatic current injection. They suggested that inhibition in cortex cannot prevent the firing of a neuron receiving strong excitatory input. In con

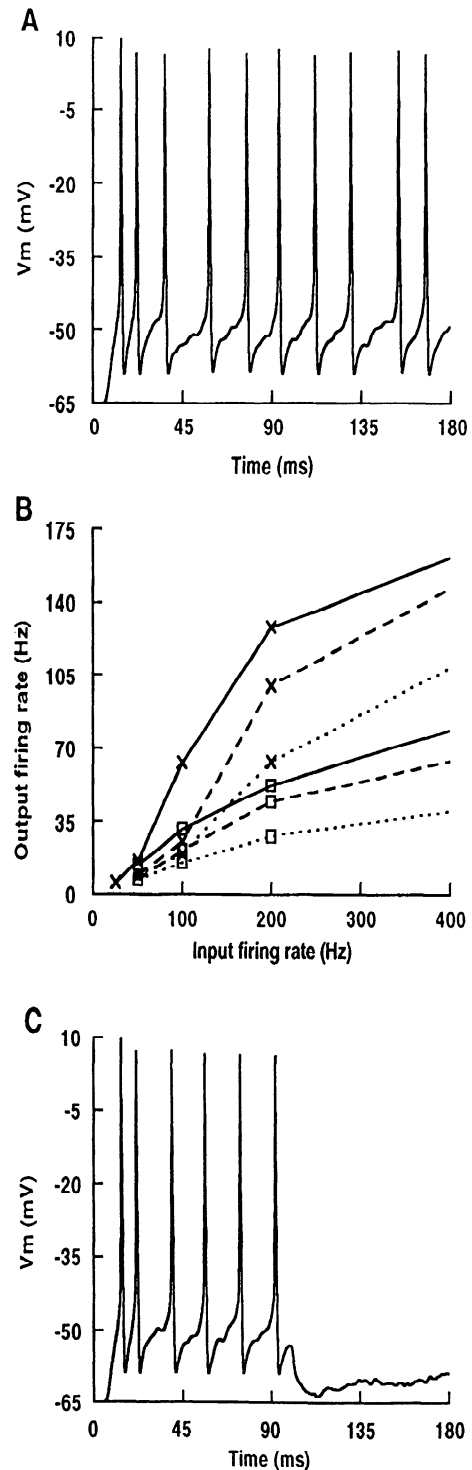


FIG. 5. Effect of inhibition on firing rate of synaptically activated model layer 2 pyramid. *A*: adapting train of action potentials produced by 70 excitatory inputs active at a mean frequency of 200 Hz. *B*: firing rate of model as a function of the firing rate of its 70 excitatory inputs.  $\times$ , initial, peak firing rate;  $\square$ , steady, adapted firing rate. Solid traces are results without inhibition. Dashed traces are results with 33 additional, inhibitory synapses firing at 100 Hz. This level of inhibition has little effect on the strongly activated pyramid. Dotted traces are results with the firing rate of the inhibitory inputs equal to twice that of the excitatory inputs in each case. This more realistic level of inhibition causes a significant decrease in the firing rate of the pyramid, although firing is not completely suppressed. *C*: firing is completely suppressed when an additional 150 somatic inhibitory inputs, firing at a mean frequency of 400 Hz at  $t = 100$  ms, are added to the simulation shown in *A*.

trast, studies *in vitro* indicate that synaptically evoked GABA<sub>A</sub> inhibition is strong enough to briefly suppress the firing of cortical neurons driven by large depolarizing current injections (Connors et al. 1988; McCormick 1989), although these results must be interpreted with caution given the large difference in GABA<sub>A</sub> conductance elicited *in vivo* and *in vitro* (Berman et al. 1989).

### *Effectiveness of inhibition*

Under what conditions could inhibition be strong enough to suppress firing? What is the effect of strong synaptic activation on  $R_{in}$  of the target neuron? These have been the subject of previous experimental and theoretical studies (Berman et al. 1991; Douglas et al. 1988; Koch et al. 1990). To address these issues the model layer 2 pyramid was driven by the same concurrently active 70 excitatory and 33 inhibitory synapses as in Fig. 3. Active conductances were added to the model (Table 1) to produce adapting trains of action potentials (Fig. 5A). Figure 5B shows the firing rate of the model cell as a function of the firing rate of the 70 excitatory synapses. The solid traces are results obtained without any inhibition. The dashed traces are results obtained with the inhibitory firing rate fixed at 100 Hz, which corresponds to the simulations done by Douglas and Martin (1990a). The crosses are the instantaneous firing rate of the model for the first interspike interval. The boxes are the steady-state (adapted) firing rate. In agreement with Douglas and Martin, the effect of the inhibition was to increase the threshold of the neuron and only slightly reduce the firing rate above threshold.

These simulations neglect the observation that inhibition is correlated with excitation (Ferster 1986), which would occur if the inhibitory cells were being driven by the excitatory cells that they were inhibiting (Douglas and Martin 1991). It is reasonable to assume that the firing rate of the inhibitory inputs would increase with the firing rate of the pyramidal cell, and hence with the firing rate of the pyramidal cell's excitatory inputs (the 70 excitatory synapses). Therefore we repeated the above simulations, this time setting the firing rate of the inhibitory synapses to twice that of the excitatory synapses. The results, shown in Fig. 5B (dotted traces), demonstrate that inhibitory input does have the potential to significantly reduce the firing rate of the target cell. However, the firing rate of the pyramidal cell was still substantial: the inhibition produced by 33 synapses is not enough to shut off the target cell.

The simulation was repeated with the 33 somatodendritic inhibitory synapses replaced by 25 inhibitory synapses on the 1st 25  $\mu\text{m}$  of an axon initial segment consisting of 7 cylinders whose diameter tapered from 2.5 to 0.6  $\mu\text{m}$ . This is the innervation pattern characteristic of chandelier cells, a type of cortical inhibitory interneuron (Farinas and DeFelipe 1991b). Sodium and potassium spike conductances were included on the first 25  $\mu\text{m}$  at the same density as on the soma (Table 1). The results (not shown) were nearly identical to those shown in Fig. 5. Thus we found no difference between the effect of basket cell inhibition and that of chandelier cells [see also Lytton and Sejnowski (1991)]. Similar results were also obtained when using the layer 5 cell instead of the layer 2 cell (not shown).

Cortical pyramidal cells receive hundreds of inhibitory synaptic contacts on their somata and proximal dendrites (Douglas and Martin 1990b; Farinas and DeFelipe 1991a). Therefore we increased the number of active inhibitory synapses in our simulation. We found that the activity of  $\sim 200$  somatic inhibitory synapses was sufficient to prevent a cell receiving strong excitation from firing (Fig. 5C). Consequently, strong cortical inhibition is able to prevent the firing of even strongly driven pyramidal cells, contrary to previous conclusions (Douglas and Martin 1990a). Firing was completely suppressed by 200 inhibitory inputs whether  $R_m$  of the model layer 2 pyramid was 20 or 100  $\text{k}\Omega\text{cm}^2$ . When  $R_m$  was 5  $\text{k}\Omega\text{cm}^2$ , the resting  $R_{in}$  of the model cell was so low ( $\sim 35 \text{ M}\Omega$ ) that the 70 excitatory inputs did not drive the cell very strongly and the activity of just 33 inhibitory inputs was sufficient to suppress firing.

The inhibition produced by the activity of 200 inhibitory inputs caused a huge decrease in  $R_{in}$  of the model neuron. Large decreases in  $R_{in}$  were not seen *in vivo* during nonpreferred responses or sustained hyperpolarizations (Berman et al. 1991; Douglas et al. 1988; Ferster and Jagadeesh 1992). Thus intracortical inhibition has the potential to shut off the firing of even strongly activated neurons, but this type of (shunting) inhibition has not yet been observed in cortical neurons. A possible reason for this is suggested in the DISCUSSION.

Previous simulations have shown that  $R_{in}$  of a neuron must decrease by a significant amount to prevent the cell from firing (Koch et al. 1990). However, as mentioned above, a number of recent experimental tests have shown that  $R_{in}$  shows no significant reduction during the nonpreferred response or even during sustained hyperpolarizations that are part of an optimal response to a visual stimulus (Berman et al. 1991; Douglas et al. 1988; Ferster and Jagadeesh 1992). Tests of our model show that  $R_{in}$  decreased by a significant amount during the synaptic activation used in the above simulations (Fig. 6). Thus, if we consider decrease in  $R_{in}$  as an assay for inhibition, the level of inhibition used in the simulations shown in Figs. 3 and 5B was as least as great as the level of inhibition occurring during nonpreferred or hyperpolarizing visual responses. This inhibition was not strong enough to counter significant synaptic excitation (Fig. 5B). This is further evidence that the level of inhibition that occurs during nonpreferred responses is not enough to prevent the cell from firing. It is likely that a lack of excitatory drive is what prevents the cell from firing during nonpreferred responses (Berman et al. 1991; Ferster 1986).

Table 2 shows the percentage decrease in  $R_{in}$  caused by weak and strong synaptic input. The input firing rate shown is for the 70 excitatory synapses and 33 inhibitory synapses active at twice these rates. The decrease in  $R_{in}$  was calculated relative to  $R_{in}$  at rest in the steady state as determined by current injections many times  $\tau_m$  in duration. The decreases in  $R_{in}$  produced by even weak synaptic input were above the experimentally detectable threshold (Berman et al. 1991) for all values of  $R_m$  and  $R_i$ . We found that approximately one-half of the decrease in  $R_{in}$  was due to excitatory, and one-half to inhibitory, synaptic conductance changes. This is not surprising because the individual synaptic conductances were equal, and there were about twice as many

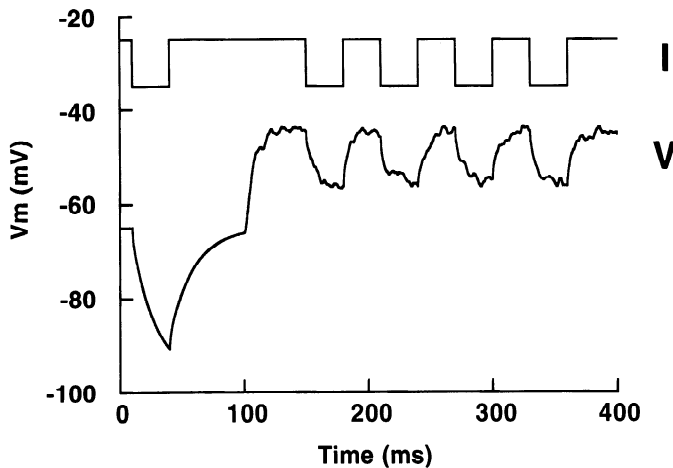


FIG. 6. Decrease in input resistance of model layer 2 pyramidal cell during synaptic activation. At 100 ms, 70 excitatory synapses and 33 inhibitory synapses were activated at 200 and 400 Hz, respectively. *Top trace*: current injected into model soma [ $-0.3$  nA each 30-ms pulse, to conform with protocol of Berman et al. (1991)]. *Bottom trace*: voltage response of model. Size of voltage deflection to each pulse gives measure of input resistance of cell. Voltage deflection is significantly smaller during synaptic activation (last 4 pulses) than at rest (1st pulse). Decrease in input resistance is actually larger than measured here, because cell is not fully charged by the pulse at rest but is fully charged by the pulses during synaptic activation. This is due to the cell's smaller time constant during synaptic activation. Data in Table 2 are calculated with the use of the real (steady-state) input resistance of the cell.

excitatory synapses, but they fired at one-half the rate of the inhibitory synapses. As noted above, the simulations of the experiments of Ferster and Jagadeesh (1992) showed that up to 20% of the EPSP reduction was due to decreases in  $R_{in}$ , even when no inhibition was present (see DISCUSSION). That excitatory input alone can cause significant decreases in  $R_{in}$  is apparent from considering the fact that the peak conductance of just one excitatory input (0.5 nS) is an appreciable fraction of the input conductance of a neuron (which for our model layer 2 pyramid ranged from 1.9 to 34.8 nS, depending on  $R_m$  and  $R_i$ ).

## DISCUSSION

### Saturation

Recent simulations of reconstructed neocortical pyramidal cells show electrotonic compactness of the basal dendrites and oblique dendrites (lateral branches from the apical trunk) over a wide range of parameter values (Holmes and Woody 1989; Stratford et al. 1989). Dendritic branches are quite isolated from each other and have high input impedances relative to the soma (Rinzel and Rall 1974). Inputs on the same branch may interact nonlinearly because synaptic currents and voltages depend on the local membrane potential and  $R_{in}$ , respectively, and these in turn both depend on local synaptic activity (Barrett and Crill 1974; Rall 1964, 1967). Synaptic input could act to reduce the excitatory driving force and  $R_{in}$ , leading to a saturation of simultaneous and subsequent excitatory input.

In confirmation, our simulations of the experiments of Ferster and Jagadeesh (1992) have provided evidence for two contributions to dendritic saturation: a reduction in driving force and a reduction in  $R_{in}$  (shunting). Based on

Eq. 1 for the membrane current, applied to voltage-independent synaptic conductances, these two components can be represented analytically in the equation for the peak synaptic potential,  $\Delta V$ , produced by  $n$  synapses each with their own reversal potential,  $V_r^i$ , undergoing conductance change  $\Delta g^i$  on a single compartment with resting membrane potential  $V_L$

$$\Delta V = \frac{(V_r - V_L)\Delta g}{(g_L + \Delta g)} \quad (2)$$

where

$$V_r = \frac{\sum_i V_r^i \Delta g^i}{\Delta g}$$

$$\Delta g = \sum_i \Delta g^i$$

and  $g_L$  is the leak conductance. The numerator in Eq. 2 represents the driving force, and the denominator gives the shunting effect. The composite synaptic event is equivalent to a single synapse with a reversal potential  $V_r$  that is a weighted sum of the individual reversal potentials and a conductance equal to the sum of the individual conductances.

All of the results we have described regarding saturation of excitatory input, effectiveness of inhibition and changes in  $R_{in}$  were consistent across a wide range of values for  $R_m$  and  $R_i$  (Table 2, Fig. 3D). The largest value for  $R_m$  we considered (100  $k\Omega cm^2$ ) seemed unlikely to occur in vivo. This value produced a value for  $R_{in}$  of  $>500$  M $\Omega$  for the model layer 2 pyramidal cell, which is well outside the range reported thus far for in vivo cortical neurons (Douglas et al. 1991; Ferster and Jagadeesh 1992; Pei et al. 1991). This value for  $R_m$  also gave a value for  $\tau_m$  of 100 ms. Such a large time constant seems incompatible with neuronal processes occurring on the time scale of tens of milliseconds (Gray et al. 1992). In performing the simulations shown in Fig. 3, with a  $\tau_m$  of 100 ms, the relative timing of all events had to be increased severalfold because the model neuron took hundreds of milliseconds to reach a steady state in response to any stimulus. If cortical neurons do have a fundamental  $R_m$  of 100  $k\Omega cm^2$ , the effective  $R_m$  of in vivo neurons is likely to be much lower because of the effect of background synaptic input (Bernander et al. 1991) (see METHODS).

A number of simulations were performed with excitatory synaptic inputs on the heads of explicitly modeled spines. The results were not significantly different from those obtained with inputs made directly onto dendritic shafts (Fig. 2). The reason for this is that the spine stem resistance (255 M $\Omega$  for our spines) is small compared with the inverse of the peak synaptic conductance (2 G $\Omega$ ) (Jaslove 1992), so

TABLE 2. Percentage decrease in  $R_{in}$  during concurrent synaptic excitation and inhibition

$R_m$ , $k\Omega cm^2$	5	5	20	20	100	100
Input firing rate, Hz	50	400	50	400	50	400
$R_i$ , $\Omega cm$						
70	16.0	41.5	42.3	74.2	82.6	94.2
200	15.3	39.2	45.5	72.6	78.1	91.9
500	15.1	37.6	39.5	70.0	80.0	91.8

that nearly all the current entering the spine head flows into the dendritic shaft (the membrane conductance of the spine is negligible). There are, however, circumstances when the differences between spine and shaft synaptic input can become significant (Qian and Sejnowski 1989; Zador et al. 1990).

### *Synaptic excitation*

Although this study was based on simulations of single neocortical pyramidal neurons, the results can be used to infer some of the principles of operation of the circuits in the neocortex. One such principle, proposed 10 years ago on the basis of physiological evidence, is that a single synapse is ineffective in firing another cell (Abeles 1982). Because one pyramidal cell makes on average only one or two synaptic contacts onto each of its targets (Braitenberg and Schuz 1991; Gabbot et al. 1987) and the vast majority of cortical synapses are pyramidal-pyramidal contacts (White 1989), the effect of a single neocortical pyramid on another is almost negligible—certainly not enough to drive the post-synaptic cell by itself (Abeles 1982). In our simulations a single synapse firing at a mean frequency of 100 Hz produced a somatic depolarization of  $<1$  mV. Maximally activating a whole dendritic segment (depolarizing to 0 mV with the use of current injection) was not enough to drive the cell to fire at the rates observed during visual stimulation.

Thus there must be convergence of synaptic inputs from many cells to produce significant firing (Douglas and Martin 1990b). How many? Our model cells required tens of synapses, active within an interval of a few milliseconds, to reach threshold. Firing at the rates observed during visual stimulation required about a hundred synapses active at a few hundred hertz. The saturation demonstrated in Fig. 3 indicates that the additional activation of more synapses has a decreasing effect. Because the maximum firing rates we used for our inputs were at the upper limits of sustained firing rates in cortex, it is likely that maximal firing will require the activity of a few hundred presynaptic cells, as suggested for the hippocampus (Andersen et al. 1990; Miles and Wong 1986; Sayer et al. 1990), spinal cord (Jack et al. 1981; Walmsley et al. 1987), and cerebellum (Rapp et al. 1992). If the inputs were completely synchronous, a high-frequency discharge could be evoked by a few tens of active synapses (Abeles 1982; Bush and Douglas 1991). This “dynamic range” of a few tens to a few hundred active inputs is only a small fraction of the thousands of synapses on a single pyramidal neuron (Douglas and Martin 1990b). This implies that a pyramidal cell can be driven by any one of several different groups of presynaptic cells, allowing the same neuron to participate in many (possibly independent) processes.

If passive membrane is assumed, a single EPSP with peak conductance 0.5 nS on the model layer 2 cell produced a somatic depolarization with a peak amplitude approximately twice that seen in the layer 5 cell. This is because  $R_{in}$  of the layer 2 cell (with the same  $\tau_m$ ) is approximately twice that of the layer 5 cell. We have found that twice as many excitatory synapses were needed to drive the layer 5 cell to fire at the same frequency as the layer 2 cell. This fits with

the observation that large layer 5 pyramids have about twice the number of spines as small layer 2 pyramids. However, there is as yet no experimental evidence that single EPSPs are larger in layer 2 cells than in layer 5 cells.

### *Synaptic inhibition*

The 33 inhibitory synapses used in the simulations of Fig. 3, *C* and *D*, are a fraction of the several hundred that exist on the soma and proximal dendrites of each pyramidal cell (Douglas and Martin 1990b; Farinas and DeFelipe 1991a). The activity of this small fraction was not sufficient to prevent the firing of a cell receiving strong excitation (Fig. 5*B*), yet it was enough to reduce  $R_{in}$  significantly (Fig. 6, Table 2). Because  $R_{in}$  does not decrease during nonpreferred or hyperpolarizing responses to visual stimuli (Berman et al. 1991; Douglas et al. 1988; Ferster and Jagadeesh 1992), we agree with Berman et al. (1991) that inhibition in the cortex (at least primary visual cortex) does not act to counter sustained ( $>50$ – $100$  ms) excitation.

What then is the role of inhibition? Inhibition is correlated with excitation (Ferster 1986); thus maximal inhibitory activity is expected during the periods of maximum firing caused by excitatory input. This statement may seem paradoxical, but only if the excitation and inhibition are considered as simultaneous and sustained, without any temporal structure. However, analysis of inhibitory activity during visual stimulation [Fig. 14 of Lytton and Sejnowski (1991)] reveals that compound IPSPs can occur rhythmically rather than randomly. This might be produced by feedback inhibition generated in response to stimulation by the same excitatory cells that the inhibition targets (Douglas and Martin 1991). It has been shown that such a system can produce synchronization of excitatory and inhibitory populations and consequent rhythmic IPSPs (Bush and Douglas 1991). Compound EPSPs are also rhythmic in this model but are out of phase with the IPSPs. In fact, it is the compound IPSP generated by the compound EPSP that terminates the burst of firing in the pyramidal cells and ensures synchronization (Bush and Douglas 1991).

The activity of hundreds of inhibitory synapses would be required to generate an IPSP capable of shutting off the firing of the pyramidal cells. In our simulations the simultaneous activity of  $\sim 200$  inhibitory synapses prevented the firing of our model cells despite strong synaptic excitation. Such a compound IPSP would produce a very large decrease in  $R_{in}$  of the target cell, but the decrease would be transient (of order 10 ms) because the inhibitory cells stop firing when no longer driven by the pyramids they inhibit. Transient conductance changes cannot be detected by current pulse injection (Berman et al. 1991), but it might be possible to sample the peak slope conductance at different membrane potentials. Thus we suggest that the role of inhibition is to synchronize the firing of groups of pyramidal cells by rhythmically turning on transiently but powerfully during optimal stimulation [see also Lytton and Sejnowski (1991), who considered the efficacy of lower frequency inhibitory inputs to entrain pyramidal cells]. Our proposal reconciles the fact that effective inhibition (preventing firing of target) must cause a large decrease in  $R_{in}$

with the fact that such decreases in  $R_{in}$  have not been seen in vivo.

There has been very little experimental study of changes in  $R_{in}$  during the response to optimal stimulation. Such experiments are hard to perform and interpret because of the large, rapid fluctuations in membrane potential and large suprathreshold intrinsic voltage-dependent conductance changes occurring during these periods. Existing data show input conductance increases of up to 40% during optimal stimulation (Berman et al. 1991). Our results indicate that  $R_{in}$  should decrease substantially during optimal stimulation, but, as with inhibition, the detectability of this decrease using current pulses would depend on how much of the excitatory input is transient and how much is sustained.

The inhibition discussed in the above argument is assumed to be GABA<sub>A</sub> inhibition. The slower, hyperpolarizing GABA<sub>B</sub> inhibition probably has a different role that could be investigated with the use of a network simulation [for one suggestion see Abbott (1991)]. In a realistic network the temporal structure of synaptic inputs would be much closer to in vivo conditions than the random inputs used here. This would allow better estimates of the numbers of inputs driving a pyramidal cell and a better way to study the role of inhibition.

Our conclusion that inhibition does not act as a veto of sustained excitation is in agreement with Berman et al. (1991). We have also replicated their results showing that a modest level of inhibition does not prevent the firing of its target (Douglas and Martin 1990a). However, using revised assumptions about the amount of inhibition impacting on a single pyramidal neuron, we have shown that a stronger level of inhibition can shut off the firing of a strongly driven target cell. We reconcile these results by postulating that such strong inhibition is only activated transiently, during periods of maximum excitatory activity.

### Conclusions

Neocortical pyramidal cells do not linearly integrate synaptic input, even in the absence of active membrane properties. Despite the electrotonic compactness of pyramidal basal/oblique dendritic trees, saturation of excitatory input is a real phenomenon that places a sharp limit on the number of active excitatory inputs that can contribute to the response of a particular pyramidal cell.

Cortical inhibition can in principle suppress the firing of its targets, but a role for inhibition as a negator of inappropriate excitatory input is not consistent with experimental data and theoretical studies. Both data and models lead to the view that excitation and inhibition are a synergistic pair of processes combining coactively to shape the response of a cortical neuron to optimal stimuli (Berman et al. 1991; Bush and Douglas 1991).

We thank R. J. Douglas and K. A. C. Martin for providing us with the cortical cell morphologies, I. Segev for comments on the manuscript, and D. Ferster for a number of useful discussions.

Support was provided by The Howard Hughes Medical Institute and The National Institute for Mental Health.

Address for reprint requests: P. C. Bush, CNL, Salk Institute, 10010 N. Torrey Pines, La Jolla, CA 92037.

Received 7 September 1993; accepted in final form 1 February 1994.

### REFERENCES

- ABBOTT, L. Firing-rate models for neural populations. In: *Neural Networks: From Biology to High-Energy Physics. Proceedings*, edited by O. Benhar, C. Bosio, P. Del Giudice, and E. Taber. Pisa: ETS Edrifice 1991.
- ABELES, M. *Local Cortical Circuits: An Electrophysiological Approach*. Berlin: Springer-Verlag, 1982.
- ANDERSEN, P., RAASTAD, M., AND STORM, J. F. Excitatory synaptic integration in hippocampal pyramids and dentate granule cells. *Symp. Quant. Biol.* 55: 81–86, 1990.
- BARRETT, J. N. AND CRILL, W. E. Influence of dendritic location and membrane properties on the effectiveness of synapses on cat motoneurons. *J. Physiol. Lond.* 293: 325–345, 1974.
- BERMAN, N. J., DOUGLAS, R. J., AND MARTIN, K. A. C. The conductances associated with inhibitory postsynaptic potentials are larger in visual cortical neurons in vitro than in similar neurons in intact, anaesthetized rats (Abstract). *J. Physiol. Lond.* 418: 107P, 1989.
- BERMAN, N. J., DOUGLAS, R. J., MARTIN, K. A. C., AND WHITTERIDGE, D. Mechanisms of inhibition in cat visual cortex. *J. Physiol. Lond.* 440: 697–722, 1991.
- BERNANDER, O., DOUGLAS, R. J., MARTIN, K. A. C., AND KOCH, C. Synaptic background activity influences spatiotemporal integration in single pyramidal cells. *Proc. Natl. Acad. Sci. USA* 88: 11569–11573, 1991.
- BONDS, A. B. Role of inhibition in the specification of orientation selectivity of cells in the cat striate cortex. *Visual Neurosci.* 2: 41–55, 1989.
- BORG-GRAHAM, L. J. *Modeling the Somatic Electrical Response of Hippocampal Pyramidal Neurons*. Cambridge, MA: MIT, 1987.
- BRAITENBERG, V. AND SCHUZ, A. *Anatomy of the Cortex*. Berlin: Springer-Verlag, 1991.
- BUSH, P. C. AND DOUGLAS, R. J. Synchronization of bursting action potential discharge in a model network of neocortical neurons. *Neural Comp.* 3: 19–30, 1991.
- BUSH, P. C. AND SEJNOWSKI, T. J. Simulations of a reconstructed cerebellar Purkinje cell based on simplified channel kinetics. *Neural Comp.* 3: 299–309, 1991.
- CONNORS, B. W., MALENKA, R. C., AND SILVA, L. R. Two inhibitory postsynaptic potentials, and GABA<sub>A</sub> and GABA<sub>B</sub> receptor-mediated responses in neocortex of rat and cat. *J. Physiol. Lond.* 406: 443–468, 1988.
- DOUGLAS, R. J. AND MARTIN, K. A. C. Control of neuronal output by inhibition at the axon initial segment. *Neural Comp.* 2: 283–292, 1990a.
- DOUGLAS, R. J. AND MARTIN, K. A. C. Neocortex. In: *Synaptic Organization of the Brain*, edited by G. Shepherd. New York: Oxford Univ. Press, 1990b, p. 220–248.
- DOUGLAS, R. J. AND MARTIN, K. A. C. A functional microcircuit for cat visual cortex. *J. Physiol. Lond.* 440: 735–769, 1991.
- DOUGLAS, R. J. AND MARTIN, K. A. C. Exploring cortical microcircuits: a combined anatomical, physiological, and computational approach. In: *Single Neuron Computation*, edited by T. McKenna, J. Javis, and S. F. Zornetzer. San Diego, CA: Academic, 1992.
- DOUGLAS, R. J., MARTIN, K. A. C., AND WHITTERIDGE, D. Selective responses of visual cortical cells do not depend on shunting inhibition. *Nature Lond.* 332: 642–644, 1988.
- DOUGLAS, R. J., MARTIN, K. A. C., AND WHITTERIDGE, D. An intracellular analysis of the visual responses of neurones in cat visual cortex. *J. Physiol. Lond.* 440: 659–696, 1991.
- FARINAS, I. AND DEFELIPE, J. Patterns of synaptic input on corticocortical and corticothalamic cells in the cat visual cortex. I. The cell body. *J. Comp. Neurol.* 304: 53–69, 1991a.
- FARINAS, I. AND DEFELIPE, J. Patterns of synaptic input on corticocortical and corticothalamic cells in the cat visual cortex. II. The axon initial segment. *J. Comp. Neurol.* 304: 70–77, 1991b.
- FERSTER, D. Orientation selectivity of synaptic potentials in neurons of cat primary visual cortex. *J. Neurosci.* 6: 1284–1301, 1986.
- FERSTER, D. AND JAGADEESH, B. EPSP-IPSP interactions in cat visual cortex studied with in vivo whole-cell patch recording. *J. Neurosci.* 12: 1262–1274, 1992.
- GABBOT, P. L. A., MARTIN, K. A. C., AND WHITTERIDGE, D. Connections between pyramidal neurons in layer 5 of cat visual cortex (area 17). *J. Comp. Neurol.* 259: 364–381, 1987.
- GRAY, C. M., ENGEL, A. K., KOENIG, P., AND SINGER, W. Synchronization of oscillatory neuronal responses in cat striate cortex: temporal properties. *Visual Neurosci.* 8: 337–347, 1992.

- HILLE, B. *Ionic Channels of Excitable Membranes*. Sunderland, MA: Sinauer, 1984.
- HINES, M. L. A program for simulation of nerve equations with branching geometries. *Int. J. Biomed. Comp.* 24: 55-68, 1989.
- HOLMES, W. R. AND WOODY, C. D. Effects of uniform and non-uniform synaptic 'activation distributions' on the cable properties of modeled cortical pyramidal neurons. *Brain Res.* 505: 12-22, 1989.
- JACK, J. J. B., NOBLE, D., AND TSJEN, R. W. *Electric current flow in excitable cells*. Oxford, UK: Oxford Univ. Press, 1975.
- JACK, J. J. B., REDMAN, S. J., AND WONG, K. The components of synaptic potentials evoked in cat spinal motoneurons by impulses in single group Ia afferents. *J. Physiol. Lond.* 321: 65-96, 1981.
- JASLOVE, S. W. The integrative properties of spiny distal dendrites. *Neuroscience* 47: 495-519, 1992.
- KISVARDY, Z. F. AND EYSEL, U. T. Functional and structural topography of horizontal inhibitory connections in cat visual cortex. *Eur. J. Neurosci.* 5: 1558-1572, 1993.
- KOCH, C., DOUGLAS, R., AND WEHMEIER, U. Visibility of synaptically induced conductance changes: theory and simulations of anatomically characterized cortical pyramidal cells. *J. Neurosci.* 10: 1728-1744, 1990.
- KOCH, C., POGGIO, T., EDELMAN, G. M., GALL, W. E., AND COWAN, W. M. Biophysics of computation: neurons, synapses, and membranes. In: *Synaptic Function*, edited by G. M. Edelman, W. E. Gall, and W. M. Cowan. New York: Wiley, 1987, p. 637-698.
- LYTTON, W. W. AND SEJNOWSKI, T. J. Simulations of cortical pyramidal neurons synchronized by inhibitory interneurons. *J. Neurophysiol.* 66: 1059-1079, 1991.
- MAJOR, G., LARKMAN, A. U., AND JACK, J. J. B. Constraining non-uniqueness in passive electrical models of cortical pyramidal neurons (Abstract). *J. Physiol. Lond.* 430: 61P, 1990.
- MARTIN, K. A. C. From single cells to simple circuits in the cerebral cortex. *Q. J. Exp. Physiol.* 73: 637-702, 1988.
- MASON, A., NICOLL, A., AND STRATFORD, K. Synaptic transmission between individual pyramidal neurons of the rat visual cortex in vitro. *J. Neurosci.* 11: 72-84, 1991.
- MCCORMICK, D. A. GABA as an inhibitory neurotransmitter in human cerebral cortex. *J. Neurophysiol.* 62: 1018-1027, 1989.
- MCCORMICK, D. A., CONNORS, B. W., LIGHTHALL, J. W., AND PRINCE, D. A. Comparative electrophysiology of pyramidal and sparsely spiny stellate neurons of the neocortex. *J. Neurophysiol.* 54: 782-806, 1985.
- MILES, R. AND WONG, R. K. S. Excitatory synaptic interactions between CA3 neurons in the guinea pig hippocampus. *J. Physiol. Lond.* 373: 397-418, 1986.
- PEI, X., VOLGUSHEV, M., VIDYASAGAR, T. R., AND CREUTZFELDT, O. D. Whole cell recording and conductance measurements in cat visual cortex in vivo. *NeuroReport* 2: 485-488, 1991.
- QIAN, N. AND SEJNOWSKI, T. J. An electro-diffusion model for computing membrane potentials and ionic concentrations in branching dendrites, spines and axons. *Biol. Cybern.* 62: 1-15, 1989.
- RALL, W. Theoretical significance of dendritic trees for neuronal input-output relations. In: *Neural Theory and Modeling*, edited by R. Reiss. Stanford, CA: Stanford Univ. Press, 1964, p. 73-97.
- RALL, W. Distinguishing theoretical synaptic potentials computed for different soma-dendritic distributions of synaptic input. *J. Neurophysiol.* 30: 1138-1168, 1967.
- RAPP, M., YAROM, Y., AND SEGEV, I. The impact of parallel fiber background activity on the cable properties of cerebellar Purkinje cells. *Neural Comp.* 4: 518-533, 1992.
- RINZEL, J. AND RALL, W. Transient response in a dendritic neuron model for current injected at one branch. *Biophys. J.* 14: 759-789, 1974.
- SAYER, R. J., FRIEDLANDER, M. J., AND REDMAN, S. J. The time course and amplitude of EPSPs evoked at synapses between pairs of CA3/CA1 neurons in the hippocampal slice. *J. Neurosci.* 10: 826-836, 1990.
- SEGEV, I. AND RALL, W. Computational study of an excitable dendritic spine. *J. Neurophysiol.* 2: 499-523, 1988.
- SEGEV, I., RAPP, M., MANOR, Y., AND YAROM, Y. Analog and digital processing in single nerve cells: dendritic integration and axonal propagation. In: *Single Neuron Computation*, edited by T. McKenna, J. Javis, and S. F. Zornetzer. San Diego, CA: Academic, 1992, p. 173-198.
- SHELTON, D. P. Membrane resistivity estimated for the Purkinje neuron by means of a passive computer model. *Neuroscience* 14: 111-131, 1985.
- SILLITO, A. M. The contribution of inhibitory mechanisms to the receptive field properties of neurones in the striate cortex of the cat. *J. Physiol. Lond.* 250: 305-329, 1975.
- SOMERS, D., NELSON, S. B., AND SUK, M. Computational model of the effects of short range excitation and inhibition on orientation selectivity in visual cortex. *Soc. Neurosci. Abstr.* 19: 628, 1993.
- SPRUSTON, N. AND JOHNSTON, D. Perforated patch-clamp analysis of the passive membrane properties of three classes of hippocampal neurons. *J. Neurophysiol.* 67: 508-528, 1992.
- STALEY, K. J., THOMAS, S. O., AND MODY, I. Membrane properties of dentate gyrus granule cells: Comparison of sharp microelectrode and whole-cell recordings. *J. Neurophysiol.* 67: 1346-1358, 1992.
- STRATFORD, K., MASON, A., LARKMAN, A., MAJOR, G., AND JACK, J. The modelling of pyramidal neurons in the cat visual cortex. In: *The Computing Neuron*, edited by R. Durbin, C. Miall, and G. Mitchison. Wokingham, England: Addison-Wesley, 1989, p. 296-321.
- TANAKA, E., HIGASHI, H., AND NISHI, S. Membrane properties of guinea pig cingulate cortical neurons in vitro. *J. Neurophysiol.* 65: 808-821, 1991.
- THOMSON, A. M., GIRDLESTONE, D., AND WEST, D. C. Voltage-dependent currents prolong single-axon postsynaptic potentials in layer III pyramidal neurons in rat neocortical slices. *J. Neurophysiol.* 60: 1896-1907, 1988.
- TRAUB, R. D., WONG, R. K. S., MILES, R., AND MICHELSON, H. A model of a CA3 hippocampal pyramidal neuron incorporating voltage-clamp data on intrinsic conductances. *J. Neurophysiol.* 66: 635-650, 1991.
- WALMSLEY, B. F. R., EDWARDS, F. R., AND TRACEY, D. J. The probabilistic nature of synaptic transmission at a mammalian central synapse. *J. Neurosci.* 7: 1037-1046, 1987.
- WHITE, E. L. *Cortical Circuits*. Boston, MA: Birkhäuser, 1989.
- ZADOR, A., KOCH, C., AND BROWN, T. H. Biophysical model of a Hebbian synapse. *Proc. Natl. Acad. Sci. USA* 87: 6718-6722, 1990.